Cluster-Based Vector-Attribute Filtering for CT and MRI Enhancement

Kiwanuka, Fred N.; Wilkinson, Michael H.F.

Published in:
Proceedings of the 21st International Conference on Pattern Recognition, ICPR 2012

IMPORTANT NOTE: You are advised to consult the publisher's version (publisher's PDF) if you wish to cite from it. Please check the document version below.

Document Version
Publisher's PDF, also known as Version of record

Publication date:
2012

[Link to publication in University of Groningen/UMCG research database](#)

Cluster-Based Vector-Attribute Filtering for CT and MRI Enhancement

Fred N. Kiwanuka, Michael H.F. Wilkinson
Johann Bernoulli Institute for Mathematics and Computer Science,
University of Groningen, The Netherlands
(F.N.Kiwanuka),(m.h.f.wilkinson)@rug.nl

Abstract

Morphological attribute filters modify images based on properties or attributes of connected components. Usually, attribute filtering is based on a scalar property which has relatively little discriminating power. Vector-attribute filtering allow better description of characteristic features for 2D images. In this paper, we extend vector attribute filtering by incorporating unsupervised pattern recognition, where connected components are clustered based on the similarity of feature vectors. We show that the performance of these new filters is better than those of scalar attribute filters in enhancement of objects in medical volumes.

1. Introduction

The main aim of connected filters [8, 9] is to extract particular image features while preserving as much of the contour information as possible. These operators act by merging flat zones given some criteria, and filter an image without introducing new contours. A sub-class of connected filters are attribute filters [1, 7]. They allow filtering based on the properties or *attributes* of connected components in the image. Usually, the attribute used is a scalar value describing either size or shape properties of connected components. This works well if the desired structures can be separated easily from undesired structures [2, 3, 6, 11]. However, in many cases, a single scalar has low discriminating power.

Recently, vector-attribute filters where proposed [5, 10]. These replace the single attribute with an attribute vector, which is a feature vector describing each connected component. This allows a better discrimination of different classes of objects. These filters are based on dissimilarity measure such as Euclidean distance, components that are similar to a set of reference shapes can be preserved or removed. This as been applied when a priori knowledge of a suitable reference shape is known.

However, in 3D medical imaging a priori knowledge of target object shapes is not readily available.

In this research, we develop 3D vector-attribute filters which in do not rely on reference shapes. We adapt unsupervised pattern recognition using k-means where object classes are learned based on the similarity of patterns. In the following, vector-attribute filtering are described in Section 2. In Section 3, the implementation is described briefly. Section 4 has the performance evaluation of vector attribute filters for medical images enhancement.The conclusions are in Section 5.

2. Attribute Filters

In binary attribute filters [1], connected components are extracted from the image. Once extracted, criteria are applied, which decide to accept or to reject components based on some property of the component, which is referred to as the *attribute*. The attribute criterion in most cases has the form:

$$\Lambda(C) = (Attr(C) \geq \lambda) \quad (1)$$

with $Attr(C)$ some real valued attribute of component C, and λ the attribute threshold. Examples in 3D are volume, non-compactness, elongation, etc. [11]. After extracting the connected components using connectivity openings, a trivial filter ψ^Λ, based on Λ is applied to each, to determine which components are retained, and which to be removed. These are defined as

$$\psi^\Lambda(C) = \begin{cases} C & \text{if } \Lambda(C) \text{is true} \\ \emptyset & \text{otherwise} \end{cases} \quad (2)$$

The complete attribute filter ψ_Λ based on criterion Λ is defined as

$$\psi_\Lambda(X) = \bigcup_{x \in X} \psi^\Lambda(\Gamma_x(X)) \quad (3)$$

in which Γ_x is the connectivity opening, which returns the connected component containing point x. This is

equivalent to taking the union of all connected components which meet criterion Λ.

The simplest way to extend these filters to gray scale is through threshold decomposition. Conceptually, the principle works by thresholding the image at all possible levels then applying the binary filter to each level, and finally stacking the results. The threshold set T_h at level h can be defined as:

$$T_h(f) = \{x \in E | f(x) \geq h\}. \quad (4)$$

The gray scale variant ψ_Λ for any increasing binary filter ψ_Λ is defined as

$$\psi_\Lambda(f)(x) = \sup\{h | x \in \Psi_\Lambda(T_h(f))\} \quad (5)$$

2.1. Vector attribute Filtering

Urbach et al. [10] replaced the single attribute by a feature vector of dimensionality d. Rather than setting d thresholds, they based the criterion on dissimilarity to a reference vector $\vec{r}$, ideally obtained from some reference shape, e.g., letters from a known font [10]. Naegel and Passat [5] use Mahalanobis distance from the mean of attribute vectors of reference shapes in 2D. In 3D, obtaining reference shapes is much harder.

Here we follow a different approach. Ideally, attribute vectors of different categories of objects should occupy compact and disjoint regions in d-dimensional attribute space. Using clustering we automatically organise the huge number of connected components of all threshold sets into a much smaller number of groups. Instead of setting reference shape and correct distance threshold, the user now inspects a few clusters.

Let $\mathcal{C} = \{C_1, C_2, \ldots, C_N\}$, be set of connected components of image X where $\vec{\tau}(C_i) \in \mathbb{R}^d$ denotes the associated attribute vector. As in [10] $\vec{\tau}$ is the vector attribute function. Any crisp clustering partitions $\mathbb{R}^d$ into k disjoint sets. Partition classes are denoted as $P_j \subset \mathbb{R}^d$, $j = 1, 2, \ldots, k$. For a vector function $\vec{\tau} : \mathcal{C} \to P_j$ every $C_i \in \mathcal{C}$ lies in exactly one partition class. The cluster criterion Λ_j becomes

$$\Lambda_j(C) = (\vec{\tau}(C) \in P_j) \quad (6)$$

i.e. it returns true if the attribute vector of C lies in partition P_j. Inserting this into (2), we can draw up the cluster-based vector-attribute filter ψ_{Λ_j} as

$$\psi_{\Lambda_j}(X) = \bigcup_{x \in X} \psi^{\Lambda_j}(\Gamma_x(X)). \quad (7)$$

It is trivial to show this adheres to all the properties of vector-attribute filters.

Though any clustering method could be used, we chose k-means clustering [4] using L_2 distance as the similarity measure. This is a method of cluster analysis which aims to partition N observations into k clusters in which each observation belongs to the cluster with the nearest mean. The main advantage of k-means is that its simple and fast($O(Nkd)$) which allows it to run on large datasets.

3. Implementation

We implemented vector attribute-filtering in the C/C++ MTdemo package [11]. This uses the Max-Tree [7] data structure to compute and visualize volumetric data. The Max-Tree is used here due to its efficient attribute computation and filtering process for 3D volumes. The filtering process is separated into four stages: construction, attribute computation, filtering and restitution. After building the tree, this auxiliary data is collected for computing the node attributes. Filtering is implemented by checking whether a node, C_h^k, satisfies a given criteria in conjunction with the filtering rules [1, 5, 7, 10]. The only changes needed are replacing scalar attributes with vector attributes, simply by calling the individual scalar attribute functions several times, and replacing the filter criterion from simple thresholding to the form of (6).

4. Results and Discussion

We ran tests on a number of 3D medical volumes of different modalities. To evaluate the performance of the the different attributes in correctly clustering the different data sets various combinations of the attributes were carried out. Determining the number of clusters was a distinct problem and this was interactively determined by the user. The k that resulted in the best noise suppression and region of interest enhancement was used. This is not easy, due to the lack of ground truth. In future work we will look into automating this.

Due to space limitations not all clusters returned are shown, but rather those clusters that satisfy the filtering objective of the the data set. The images `angiolarge`, `foot`, `Chest` are courtesy of `http://www.volvis.org` while `prostate-stone` is a 3D CT data set courtesy of the Department of Radiology and Medical Imaging, University General Hospital of Alexandroupolis, Greece. We compare the new method to scalar, threshold based attribute filtering, because no reference vectors could easily be drawn up to implement the form of [10].

Angiolarge: The aim is to filter and enhance blood vessels while suppressing unwanted tissue represent-

ing noise. Scalar-attribute filtering for 3D medical images based on size attributes perform very poorly, not only failing to enhance blood vessels but also amplifying noise, shown in Fig. 1 (c). A *volume* attribute ($\lambda = 9000$) simply amplifies noise on this data set. This applies for all size attributes. However, when a clustering attribute filter is applied on the *volume* attribute, the performance is much better, as seen in Fig. 1(e). The performance of the other size attributes is also improved by using vector attributes. Its important to note that the performance improvement is irrespective of the increase in the number of attributes used. Shape based attributes like *non-compactness* always perform well on this data set even when used in scalar-attribute filters.

Prostate-stone: We want to filter out the prostate stone while suppressing all other features. Scalar-attribute filters are able to isolate the stone but they are never successful in suppressing the noise, see Fig. 1(d). The problem has been eradicated in [2] [3] by filtering using 2 attributes successively. First, a *radial moment* filter is applied to obtain Fig. 1(d), then a *volume* filter is applied to remove the remaining noise. However, using vector attributes, the result in Fig. 1(f) is obtained in a single step. This result was obtained using k-means and the *non-compactness* attribute with $k = 17$. Higher dimension of the vector up to 5 attributes was capable of isolating the stone in a single step.

Foot: Here we aim to enhance the bones but suppress the tissue. Scalar filters struggle with this task. In Fig. 2(c), the *non-compactness* attribute enhances the bones but with noise still visible. However, the vector attribute combination of exact surface area [3], fast surface area [6] and volume perfectly enhances the bones and suppresses noise as seen in Fig. 2(e).

Female Chest: The objective here is to enhance the skeleton while suppressing the tissue. From Fig. 2 the performance of regular attribute filter is seen in Fig. 2(d), the radial moment ($\beta = 3$) attribute is able to enhance the skeleton but other unwanted tissue still remains. However, a vector attribute filter of any combination of size attributes enhances the skeleton without leaving unwanted tissue, see Fig. 2(f).

Timings: Using a Core 2 Duo E8400 at 2.0 GHz, 2GB RAM machine, we ran timings for the computation of the algorithm for vector attributes up to 6 attributes for different medical images of varying sizes and gray scale levels. The timings include the computation of the attributes and the clusters. Even for very large data sets like `mrt16_angio` with 1,554,454 nodes for 6 attributes for $k = 23$: it takes 17 seconds for size based attributes and 58 seconds for shape attributes. This is faster than most users can select an optimal setting for a single attribute.
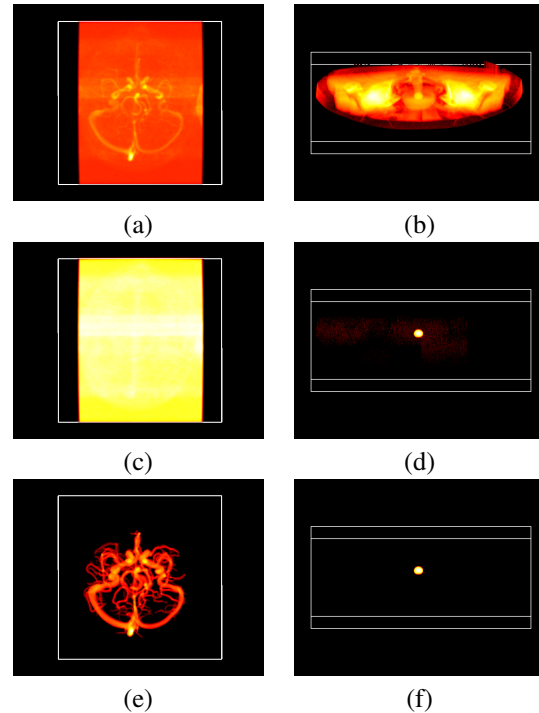

Figure 1. Left Column: (a) original (c) filtered with volume($\lambda = 9000$) (e) vector attribute filter by the same attribute using $k = 8$. Right Column: (b) original (d) filtered with radial moment ($\beta = 5, \lambda = 0.00256$) (f) vector attribute filter by the same attribute using $k = 17$.

5. Discussion and Conclusions

In this paper we presented methods for computing vector attribute filtering in 3D, using unsupervised pattern classification where features are selected or rejected based on feature vectors rather than a single property. We have shown that the unsupervised clustering of scalar or vector attributes obtain as good or better results in enhancing structures in medical images and noise suppression, than scalar-attribute filtering by manual threshold selection. These filters have much flexibility in selecting features of interest. The computational cost is modest, especially when taking the time used for manual optimisation of thresholds into account. Manual selection of clusters is simpler than threshold selection, as only a discrete number of options can be selected.

The performance of the combination of size based attributes was very good on data set that involved separating hard tissue from soft tissue that is the CT scans *foot, chest knee, prostate-stone*. While the combination of shape based attributes perform better on enhanc-
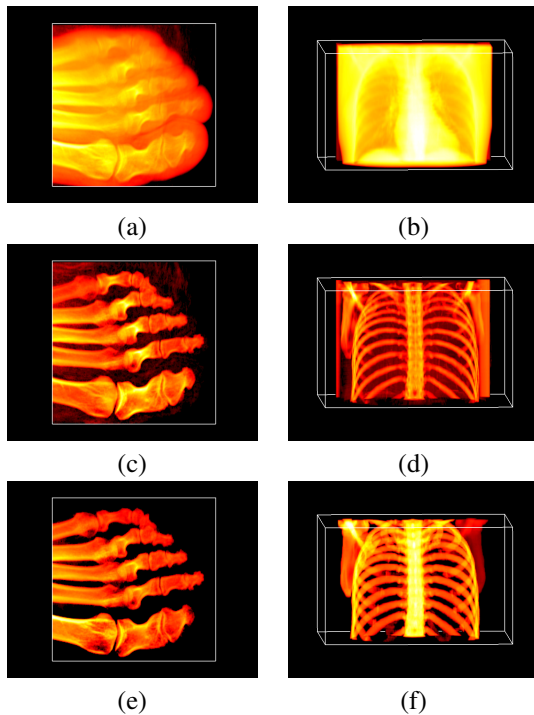
Figure 2. Foot/Female-chest: (a) original head; (c) filtered with non-compactness ($\lambda = 2.6$); (e) vector-attribute filter using $k = 9$; (b) original chest; (d) filtered with radial moment ($\beta = 3, \lambda = 0.034$); (f) vector-attribute filter using $k = 12$.

ing and noise suppression on data sets that emphasise soft tissue contrast, such as MRI volumes *angiolarge, mrt16_angio, mrt16_angio2* . The combination of size and shape attributes is biased to the size based attribute filtering. This has to do with use of the L_2 metric where the features with a large range dominate others.

The clustering of scalar attributes (i.e. $d = 1$) using a suitable number of clusters for almost all attributes and most data sets gives very good results as compared to manual threshold selection, irrespective of whether it is a shape or size based attribute. A further increment in the number of attributes to more than 6 reveals little or no changes in performance for both size and shape based attributes. This could be due to the distance used in the clustering process as the similarity measure. Normalisation or relevance learning could be used to combine features in a better way. A further problem is that we still must set k, and that the user must select the correct cluster. Selecting the correct cluster could be assisted by providing a quick rendering of each filtered result in the GUI. This could also allow selecting multiple clusters efficiently.

In future work, we will study the behaviour of vector attribute filters for higher $d \geq 10$, and explore other clustering methods like fuzzy c-means, mean shift or vector quantisation, including ways to estimate the number of clusters from the attribute distribution. Other dissimilarity measures than the L_2 distance will also be investigated. The curse of dimensionality ultimately leads us to explore dimensional reduction techniques, since its clear that not all the attributes contribute equally to the separation of the data.

References

[1] E. J. Breen and R. Jones. Attribute openings, thinnings and granulometries. *Comp. Vis. Image Understand.*, 64(3):377–389, 1996.

[2] F. Kiwanuka and M. Wilkinson. Radial moment invariants for attribute filtering in 3D. In U. Kthe, A. Montanvert, and P. Soille, editors, *Proc. Workshop on Applications of Discrete Geometry and Mathematical Morphology (WADGMM)*, pages 37–41, 2010.

[3] F. N. Kiwanuka, G. K. Ouzounis, and M. H. Wilkinson. Surface-area-based attribute filtering in 3d. In *Proceedings of the 9th ISMM '09*, pages 70–81, Berlin, Heidelberg, 2009. Springer-Verlag.

[4] J. B. Macqueen. Some methods of classification and analysis of multivariate observations. In *Proceedings of the Fifth Berkeley Symposium on Mathematical Statistics and Probability*, pages 281–297, 1967.

[5] B. Naegel, N. Passat, N. Boch, and M. Kocher. Segmentation using vector-attribute filters: Methodology and application to dermatological imaging. In *Proc. Int. Symp. Math. Morphology (ISMM) 2007*, pages 239–250, 2007.

[6] G. K. Ouzounis, S. Giannakopoulos, C. E. Simopoulos, and M. H. F. Wilkinson. Robust extraction of urinary stones from CT data using attribute filters. In *Image Processing (ICIP), 2009 16th IEEE International Conference on*, pages 2629 –2632, 2009.

[7] P. Salembier, A. Oliveras, and L. Garrido. Antiextensive connected operators for image and sequence processing. *IEEE Trans. Image Proc.*, 7:555–570, 1998.

[8] P. Salembier and J. Serra. Flat zones filtering, connected operators, and filters by reconstruction. *IEEE Trans. Image Proc.*, 4:1153–1160, 1995.

[9] P. Salembier and M. H. F. Wilkinson. Connected operators: A review of region-based morphological image processing techniques. *IEEE Signal Processing Magazine*, 26(6), 2009.

[10] E. R. Urbach, N. J. Boersma, and M. H. F. Wilkinson. Vector-attribute filters. In *Mathematical Morphology: 40 Years On, Proc. Int. Symp. Math. Morphology (ISMM) 2005*, pages 95–104, Paris, 18-20 April 2005.

[11] M. A. Westenberg, J. B. T. M. Roerdink, and M. H. F. Wilkinson. Volumetric attribute filtering and interactive visualization using the max-tree representation. *IEEE Trans. Image Proc.*, 16:2943–2952, 2007.